Wireless Pers Commun (2013) 69:1347–1364
DOI 10.1007/s11277-012-0637-z

An Unambiguous Tracking Method Based on Pseudo Correlation Function for AltBOC(15,10) Signal

Huihua Chen · Rong Wang · Weimin Jia · Jiawei Ren · Minli Yao

Published online: 24 April 2012

Abstract The Galileo E5 or COMPASS B2 signal is the most precision civil and most challenging navigation signal which will be available in the near future for regular navigation. The excellent performance of this signal was reached by Alternative Binary Offset Carrier (AltBOC) modulation, which is specially designed for high precision range measurement and which is featured by extremely wide bandwidth. However, this modulation presents some drawbacks. The most severe one is the ambiguity problem in AltBOC signal acquisition and tracking, which introduces a large bias in the pseudo-range measurement. In order to solve this problem, an unambiguous tracking method based on a pseudo correlation function for AltBOC(15,10) modulation signal is proposed in this paper. It employs two local signals and a novel combination function, which completely removes side peaks from the correlation function while keeping the sharp main peak. Impacts of multipath on the proposed method are also investigated. Simulation results demonstrate that the proposed method is totally unambiguous while exhibiting an average multipath performance with respect to the existing unambiguous tracking methods.

Keywords Global navigation satellite systems (GNSS) · Alternative binary offset carrier (AltBOC) · Unambiguous tracking · Multipath

H. Chen (✉) · R. Wang · W. Jia · J. Ren · M. Yao
Xi'an Research Institute of High Technology, Xi'an 710025, China
e-mail: chenhuihuachina@hotmail.com

W. Jia
e-mail: jwm602@163.com

J. Ren
e-mail: wdrjw@yahoo.com.cn

M. Yao
e-mail: yaominli@sohu.com

R. Wang
Department of Automation, Tsinghua University, Beijing 100084, China
e-mail: wr07@mails.tsinghua.edu.cn

Abbreviations

GNSS	Global navigation satellite systems
AltBOC	Alternative binary offset carrier
PCF	Pseudo correlation function
ACF	Autocorrelation function
CCF	Cross-correlation function
PSD	Power spectral density
SC	Side-peaks cancellation
NEML	Narrow early-minus-late

1 Introduction

The European Galileo and Chinese Compass are the new global navigation satellite systems (GNSS), which will use the novel alternative binary offset carrier (AltBOC) modulation scheme to transmit four channels in the E5/B2 band (1,164–1,219 MHz/1,166–1,217 MHz) [1,2]. This is because that the AltBOC modulation is able to carry different services on the upper and lower bands, these two sub bands can be received and processed independently to achieve performance identical to the traditional BPSK signal, or be received and processed coherently to achieve better positioning accuracy [3–6].

As reception, the multiplexing adopted for the transmission of the E5a (B2a) and E5b (B2b) signals allows three alternative receiver implementations and processing: (1) E5a (B2a) single sideband reception, (2) E5b (B2b) single sideband reception, (3) E5/B2 (or E5a + E5b/B2a + B2b) wideband reception [4]. Receiving the E5/B2 wideband can reduce the loss of signal and achieve better positioning accuracy than single sideband [4]. However, AltBOC modulation presents some drawbacks, the most severe being the ambiguity problem in tracking. Due to the sub-carriers of AltBOC modulation signal brings multiple positive and negative side-peaks for its autocorrelation function (ACF), the receiver may lock onto one of the side peaks. This would result in intolerable biased measurements for modern navigation [7,8]. Therefore, better solutions (compared with the traditional BPSK modulation case) are necessary to deal with this ambiguity.

Currently, in order to alleviate this ambiguity problem, several methods have been proposed in literature. Among them, there are two representative ways which are, respectively referred to as BPSK-like techniques and side-peaks cancellation (SC) techniques. The BPSK-like techniques remove the effect of the sub-carrier modulation, by implementing a pair of single sideband correlation receivers, which might be used individually (single sideband case, SSB) or combined non-coherently (dual sideband case, DSB) [7]. Thus each sidelobe is treated independently as a BPSK(10) signal, which provides an unambiguous correlation function and a wider S-curve steady domain. However, the BPSK-like method presents some drawbacks. Firstly, due to the filter effect, there are degradation for SSB process and DSB process. Secondly, the sharp main peak of the ACF is destroyed while removing its ambiguity, it makes the RMS bandwidth of received signal approaches to that of BPSK signal, and the robustness against multipath of the AltBOC signal is lost.

SC techniques are a kind of innovational methods to solve the ambiguity problem, which they can keep the sharp main peak [9,10]. The basic idea of SC techniques is using synthesized correlation function instead of AltBOC ACF in acquisition and tracking. The first SC technique for AltBOC signal is proposed in [7]. This approach, namely Sub Carrier Phase Cancellation (SCPC) is to get rid of the sub-carrier in the same way as carrier. An in-phase and a quadrature-phase local sub-carrier are generated, thus the received filtered signal is both correlated with the local AltBOC signal in sub-carrier phase and correlated with the local AltBOC signal in sub-carrier quadrature, then are combined, an unambiguous cross-correlation function (CCF) similar to the BPSK one is obtained. The main disadvantage of the SCPC method is that the sharp of the main peak is destroyed. For accurate delay tracking, preserving a sharp main peak of the ACF is a pre-requisite. A new unambiguous tracking technique is described in [8], namely divided correlation function (DCF), which creates new sub-carrier signals by dividing the conventional sub-carrier signals of AltBOC signals and completely removes the side-peaks of the ACF, while keeping the sharp correlation of the main peak. However, multiple correlators (e.g. 8 complex correlators at least) are utilized in this approach, which is too complex to implement in practice. Additionally, the amplitude of the main peak of this approach is an imperfect CCF and degraded seriously, so this method is limited to be used in interference channel [8,11,12]. All of the SC techniques mentioned above use new local replica signals whose chip waveforms are different from that of the received signal and non-coherently combine outputs of the correlation channels to completely remove the side peaks from the correlation function [10].

In order to solve the AltBOC signal ambiguity problem with less hardware complexity compared with DCF method. First, this paper derives an analytical expression of the CCF of two signals with step-shape chip waveforms, which is suitable for other SC techniques. Second, based on the CCF, we create a proposed pseudo correlation function (PCF), which has only one ideal triangular main peak with no side peaks for tracking via designing the chip waveforms of local signal. Third, an unambiguous tracking method based on the proposed PCF for AltBOC(15,10) modulation signals is given out. This method is convenient to implement and requires the same number of complex correlators as SCPC method (4 complex correlators).

The remainder of this paper is organized as follows. In Sect. 2, the concept, some main characteristics and ambiguity problem of the AltBOC modulation signal are described. Section 3 explains the essence of the proposed method as well as its theoretical formulation while Sect. 4 investigates the impact of the most significant disturbance (multipath) on code tracking using the new proposed method. And finally conclusions are drawn in Sect. 5.

2 AltBOC(15,10) Modulation Signal

2.1 Definitions and Main Characteristics

The Galileo E5 or Compass B2 signals employ a complex sub-carrier modulation known as AltBOC(15,10) modulation, whose center frequency is 1,191.795 MHz, has a lower main split lobe at 1,176.45 MHz and an upper main split lobe at 1,207.14 MHz. Taking Galileo system as example, Four channels (E5a-I, E5a-Q, E5b-I, E5b-Q) will be transmitted in the E5 band by each Galileo satellite taking advantage of the AltBOC modulation. E5a-I and E5b-I are the so-called data channels, whereas the other two are named pilot channels. Similar to the BOC modulation, AltBOC modulation is normally expressed as AltBOC(m, n) in the navigation community, where m is the ratio of the sub-carrier frequency f_s to 1.023 MHz, and n denotes the ratio of the spreading code rate f_c to 1.023 MHz. m and n are both constrained to positive integer, $m \geq n$, and the ratio $M = 2m/n$ is a positive integer [1–3].

When we analyzed the AltBOC modulation, having a constant envelope is a must since otherwise the distortion caused by the High Power Amplifier (HPA) in the satellite would not be tolerable [4,13,14]. AltBOC(m, n) modulation signal adopts a 4-level sub-carrier waveform whose baseband transition rate is 8 times of the sub-carrier frequency, and product terms are also added to maintain a constant envelope when 4 different Pseudo Noise (PN) codes are used. A detailed description of the generation of the AltBOC(m, n) modulated signal with constant envelope can be found in [4,13,14]. The analytical expression of the AltBOC(m, n) modulated signal $s_{\text{AltBOC}}^{\text{C}}(t)$ is given as:

$$\begin{aligned} s_{\text{AltBOC}}^{\text{C}}(t) = & \left(c_L^D + jc_L^P\right)\left[sc_d(t) - jsc_d\left(t - \frac{T_s}{4}\right)\right] \\ & + \left(c_U^D + jc_U^P\right)\left[sc_d(t) + jsc_d\left(t - \frac{T_s}{4}\right)\right] \\ & + \left(\overline{c_L^D} + j\overline{c_L^P}\right)\left[sc_p(t) - jsc_p\left(t - \frac{T_s}{4}\right)\right] \\ & + \left(\overline{c_U^D} + j\overline{c_U^P}\right)\left[sc_p(t) + jsc_p\left(t - \frac{T_s}{4}\right)\right] \end{aligned} \tag{1}$$

where the superindex of $s_{\text{AltBOC}}^{\text{C}}(t)$ indicates constant envelope, T_s is the inverse of the sub-carrier frequency. And the useful signal components are expressed as:

$$\begin{aligned} c_L^D &= d_L(t)\, c_{L-d}(t) = \text{the E5a-I (B2a-I) signal component} \\ c_L^P &= c_{L-p}(t) = \text{the E5a-Q (B2a-Q) signal component} \\ c_U^D &= d_U(t)\, c_{U-d}(t) = \text{the E5b-I (B2b-I) signal component} \\ c_U^P &= c_{U-p}(t) = \text{the E5b-Q (B2b-Q) signal component.} \end{aligned} \tag{2}$$

The respective dashed signal components $\overline{c_L^D}$, $\overline{c_L^P}$, $\overline{c_U^D}$, and $\overline{c_U^P}$, are product signals according to the following equations:

$$\overline{c_L^D} = c_U^P c_U^D c_L^P;\ \overline{c_L^P} = c_U^D c_U^P c_L^D;\ \overline{c_U^D} = c_L^D c_U^P c_L^P;\ \overline{c_U^P} = c_U^D c_L^D c_L^P. \tag{3}$$

The data and pilot sub-carriers (chip waveform) are expressed as:

$$\begin{cases} sc_d(t) = \frac{\sqrt{2}}{4}\text{sign}\left[\cos\left(2\pi f_s t - \frac{\pi}{4}\right)\right] + \frac{1}{2}\text{sign}\left[\cos\left(2\pi f_s t\right)\right] \\ \qquad\quad + \frac{\sqrt{2}}{4}\text{sign}\left[\cos\left(2\pi f_s t + \frac{\pi}{4}\right)\right] \\ sc_P(t) = -\frac{\sqrt{2}}{4}\text{sign}\left[\cos\left(2\pi f_s t - \frac{\pi}{4}\right)\right] + \frac{1}{2}\text{sign}\left[\cos\left(2\pi f_s t\right)\right] \\ \qquad\quad - \frac{\sqrt{2}}{4}\text{sign}\left[\cos\left(2\pi f_s t + \frac{\pi}{4}\right)\right]. \end{cases} \tag{4}$$

The main property of the modulated signals is related to the ACF, which determines the acquisition and tracking abilities. The analytical expression of ACF for the constant envelope AltBOC(m, n) modulation signal can be obtained from [13,14]:

$$\begin{aligned} R_{\text{AltBOC}}^{\text{C}}(\tau) = & R_{c_L^D sc_d}(\tau) + R_{c_L^D sc_d'}(\tau) + R_{c_L^P sc_d}(\tau) + R_{c_L^P sc_d'}(\tau) + \\ & R_{c_U^D sc_d}(\tau) + R_{c_U^D sc_d'}(\tau) + R_{c_U^P sc_d}(\tau) + R_{c_U^P sc_d'}(\tau) + \\ & R_{\overline{c_L^D} sc_p}(\tau) + R_{\overline{c_L^D} sc_p'}(\tau) + R_{\overline{c_L^P} sc_p}(\tau) + R_{\overline{c_L^P} sc_p'}(\tau) + \\ & R_{\overline{c_U^D} sc_p}(\tau) + R_{\overline{c_U^D} sc_p'}(\tau) + R_{\overline{c_U^P} sc_p}(\tau) + R_{\overline{c_U^P} sc_p'}(\tau). \end{aligned} \tag{5}$$

This ACF without front-end filter is shown in Fig. 1 along with the normalized BPSK(10) ACF.

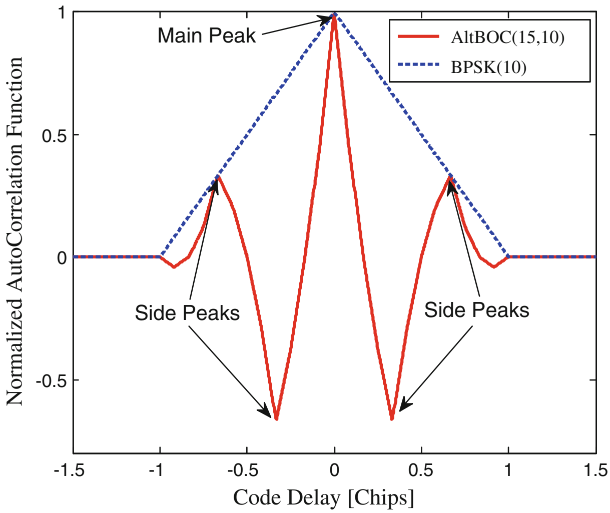

Fig. 1 Normalized ACFs for AltBOC(15,10) and BPSK(10) signals

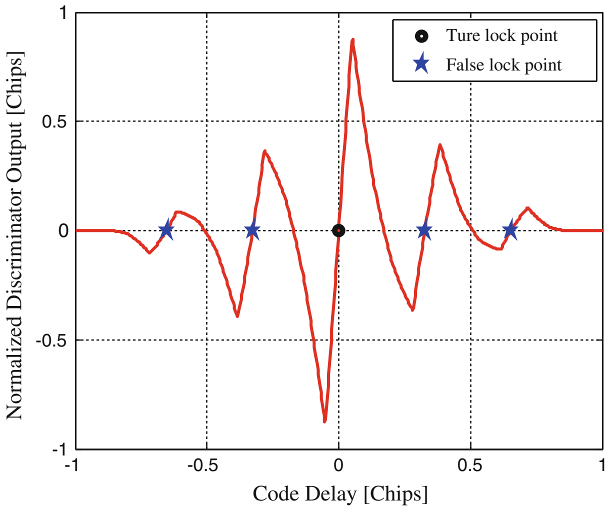

Fig. 2 Ambiguity problem in AltBOC(15,10) signal tracking

2.2 Ambiguity Problem

As shown in Fig. 1, it can be seen that the ACF of AltBOC(15,10) has one main peak with multiple side peaks. Compared with the triangular ACF of BPSK(10) signals, the ACF of AltBOC signals has sharper main peak, which means better tracking accuracy. However, when using a traditional narrow early-minus-late (NEML) tracking loop, the discriminator characteristic curve of AltBOC(m, n) signal has $4\,m/n-2$ stable false lock points which are due to side peaks of the ACF. Then it is possible to have the loop locking on one of the side peaks, which would result in intolerable biased measurements. This problem is reputed as the ambiguity problem for AltBOC signal tracking. Figure 2 shows the discriminator output for AltBOC(15,10) signal using traditional NEML tracking loop for an early-late spacing of 0.1

chips, without front-end filter. From Fig. 2, it can be seen that there are one true lock point and four false lock points in the discriminator output. Therefore, it is necessary to remove the false lock points completely while maintaining the sharp main peak in tracking process.

SC techniques are a kind of innovational methods to solve the ambiguity problem, which they can maintain the sharp main peak. SC techniques perform the CCF between the received AltBOC modulated signal with local replica signals, whose chip waveforms are different from that of the received signal, and then non-coherently combine the outputs of the correlators to remove the side peaks from the correlation function [10]. Based on this concept, a newly developed method focuses specifically on AltBOC(15,10) signals and its characteristics to cope with the ambiguous tracking problem. It is described in the following section.

3 Proposed Unambiguous Tracking Method

Many SC techniques, such as SCPC method and DCF method are based on removing the side peaks from the AltBOC(15,10) signal ACF, and their drawbacks are presented in Sect. 1. Different from these SC techniques, the proposed method employs two local signals who use 'step-like' chip waveforms, which are different from the received AltBOC signal, and then non-coherently combines the output of the correlators in order to obtain a no side peaks function for tracking in the replacement of the traditional ACF.

The key of the SC techniques is to design the chip waveform of local signal, which need to be analyzed by the CCF of the signals with various step-shape chip waveform. Therefore, it is desired to define a parameterized local signal model the chip waveform of which has a high degrees of freedom and is easy to generate in receivers to provide more opportunities for waveform optimization. Currently, to the authors' knowledge, there is no available theoretical formula of the CCF between the AltBOC(m, n) signal and local signal with step-shape chip waveform. In Sect. 3.1, an analytical expression of this CCF is given out, which is the basis of the investigation of a proposed PCF in Sect. 3.2 and a newly developed proposed method in Sect. 3.3.

3.1 Derivations of CCF

To make progress in our derivations, it is necessary to analyze the data and pilot sub-carriers. In this method, these chip waveforms are all divided into M segments, each with equal length $T_s = T_c/M$, where T_c is the period of the chip waveform. Therefore, Eq. 4 can be rewritten as:

$$\begin{cases} sc_d(t) = \sum_{k=0}^{M-1}\sum_{i=0}^{4-1} s_k a_{1i} P_{T_s/4}\left(t-(i+4k)\frac{T_s}{4}\right) \\ sc'_d(t) = sc_d\left(t-\frac{T_s}{4}\right) = \sum_{k=0}^{M-1}\sum_{i=0}^{4-1} s_k a_{2i} P_{T_s/4}\left(t-(i+4k)\frac{T_s}{4}\right) \\ sc_P(t) = \sum_{k=0}^{M-1}\sum_{i=0}^{4-1} s_k a_{3i} P_{T_s/4}\left(t-(i+4k)\frac{T_s}{4}\right) \\ sc'_p(t) = sc_p\left(t-\frac{T_s}{4}\right) = \sum_{k=0}^{M-1}\sum_{i=0}^{4-1} s_k a_{4i} P_{T_s/4}\left(t-(i+4k)\frac{T_s}{4}\right) \end{cases} \tag{6}$$

where

$$P_{T_s/4}(t) = \begin{cases} 1, \ t \in [kT_s/4, (k+1)\,T_s/4] \\ 0, \ \text{others} \end{cases}. \tag{7}$$

And s_k is the projection of $sc_d(t)$ onto $P_{T_s/4}(t)$, i.e.

$$s_k = M \int_0^T sc_d(t) \sum_{i=0}^{4-1} a_{1i} P_{T_s/4}(t)\, dt. \tag{8}$$

In principle s_k, defined as coded symbol sequence, could adopt any real value. To meet the energy normalization condition of the coded symbol sequence, the coded symbol sequence must satisfy

$$\frac{1}{M} \sum_{k=0}^{M-1} s_k^2 = 1. \tag{9}$$

The parameters of $\boldsymbol{a}_1, \boldsymbol{a}_2, \boldsymbol{a}_3$ and $\boldsymbol{a}_4$ are shown as:

$$\begin{cases} \boldsymbol{a}_1 = \left[\frac{\sqrt{2}+1}{2} \frac{1}{2} - \frac{1}{2} - \frac{\sqrt{2}+1}{2} \right]^{\mathrm{T}} \\ \boldsymbol{a}_2 = \left[\frac{1}{2} \frac{\sqrt{2}+1}{2} \frac{\sqrt{2}+1}{2} \frac{1}{2} \right]^{\mathrm{T}} \\ \boldsymbol{a}_3 = \left[-\frac{\sqrt{2}-1}{2} \frac{1}{2} - \frac{1}{2} \frac{\sqrt{2}-1}{2} \right]^{\mathrm{T}} \\ \boldsymbol{a}_4 = \left[\frac{1}{2} - \frac{\sqrt{2}-1}{2} - \frac{\sqrt{2}-1}{2} \frac{1}{2} \right]^{\mathrm{T}} \end{cases}. \tag{10}$$

Since such chip waveforms look like steps, similar with [10], we expand this kind of chip waveform of AltBOC signals to the step-shape code symbol (SCS) chip waveform, and call the signal which uses this waveform the SCS signal in this paper. Therefore, the SCS signal $s_{\mathrm{SCS}}(t)$ can be defined as

$$\begin{aligned} s_{\mathrm{SCS}}(t) = {} & \left(c_L^D + jc_L^P\right) \sum_{k=0}^{M-1} \sum_{i=0}^{3} s_k \left(a_{1i} - ja_{2i}\right) P_{T_s/4} \left(t - (i+4k)\frac{T_s}{4}\right) \\ & + \left(c_U^D + jc_U^P\right) \sum_{k=0}^{M-1} \sum_{i=0}^{3} s_k \left(a_{1i} + ja_{2i}\right) P_{T_s/4} \left(t - (i+4k)\frac{T_s}{4}\right) \\ & + \left(\overline{c_L^D} + j\overline{c_L^P}\right) \sum_{k=0}^{M-1} \sum_{i=0}^{3} s_k \left(a_{3i} - ja_{4i}\right) P_{T_s/4} \left(t - (i+4k)\frac{T_s}{4}\right) \\ & + \left(\overline{c_U^D} + j\overline{c_U^P}\right) \sum_{k=0}^{M-1} \sum_{i=0}^{3} s_k \left(a_{3i} + ja_{4i}\right) P_{T_s/4} \left(t - (i+4k)\frac{T_s}{4}\right). \end{aligned} \tag{11}$$

Every SCS chip waveform can be identified by vector $\boldsymbol{S} = \left[s_0, s_1, \ldots, s_{M-1}\right]^T$ and spreading sequence rate $f_c = 1/T_c$, thus a SCS signal can be noted by $s_{\mathrm{SCS}}(t; \boldsymbol{S}; f_c)$. An AltBOC$(m, n)$ modulated signal can be considered as a special case of the SCS signals. Its coded symbol sequence is $s_k = (-1)^k, k = 0, 1, \ldots, M-1, M = 2m/n$.

Consider the two spreading signals with SCS chip waveform $s'_{\mathrm{SCS}}(t)$ and $s'_{\mathrm{SCS}}(t)$ which have the same T_c and M, while the coded symbol sequences may be different. Substituting Eq. 11 into Eq. 5, the CCF of these two SCS signals is obtained as follows, since all the codes are of the same length and they do ideally correlate as expected from ideal random codes.

$$R_{\mathrm{CCF}}(\tau) = \frac{1}{8M} \sum_{k=0}^{M-1} \sum_{i=0}^{3} \sum_{l=0}^{M-1} \sum_{j=0}^{3} \left[\begin{array}{l} s_k s'_l \left(a_{1i}a_{1j} + a_{2i}a_{2j} + a_{3i}a_{3j} + a_{4i}a_{4j}\right) \times \\ \mathrm{Tri}\left[4Mf_c\left(\tau - ((i-j) + 4(k-l))\frac{T_s}{4}\right)\right] \end{array} \right] \tag{12}$$

where

$$\mathrm{Tri}(x) = \begin{cases} 0 & , \ |x| > 1 \\ 1 - |x| \, , & |x| \leq 1 \end{cases} . \tag{13}$$

It is relatively easy to obtain a band-limited version of the CCF of these two SCS signals. Thus we have

$$R_{\mathrm{CCF}}^{\mathrm{Filter}}(\tau) = \frac{1}{8M} \sum_{k=0}^{M-1} \sum_{i=0}^{3} \sum_{l=0}^{M-1} \sum_{j=0}^{3} \left[\begin{array}{l} s_k s_l' \left(a_{1i} a_{1j} + a_{2i} a_{2j} + a_{3i} a_{3j} + a_{4i} a_{4j} \right) \times \\ R_{\mathrm{BL}} \left[4 M f_c \left(\tau - \left((i-j) + 4(k-l) \right) \frac{T_s}{4} \right) \right] \end{array} \right] \tag{14}$$

with

$$\begin{aligned} R_{\mathrm{BL}}(\tau) = & \frac{1}{\pi} (\tau + 1) \, \mathrm{Si} \left[2\pi b (\tau + 1) \right] + \frac{1}{2\pi^2 b} \cos \left[2\pi b (\tau + 1) \right] \\ & + \frac{1}{\pi} (\tau - 1) \, \mathrm{Si} \left[2\pi b (\tau - 1) \right] + \frac{1}{2\pi^2 b} \cos \left[2\pi b (\tau - 1) \right] - \frac{2\tau}{\pi} \mathrm{Si} \left[2\pi b \tau \right] \\ & - \frac{1}{\pi^2 b} \cos \left[2\pi b \tau \right] \end{aligned} \tag{15}$$

where the band limiting parameter is defined as $b = B \frac{T_c}{2m}$, B is the front-end double-sided filter bandwidth, which is expressed in Hz, and $\mathrm{Si}(t) = \int_0^t \frac{\sin x}{x} dx$.

By looking at the expression of Eqs. 12 and 14, we may conclude that changing the coded symbol sequence vector $\boldsymbol{S} = \left[s_0, s_1, \ldots, s_{M-1} \right]^T$ can change the shape of $R_{\mathrm{CCF}}(\tau)$. This is the theoretical basis of SC techniques. Therefore, we can obtain a near-perfect discriminator S-curve without false lock points by using some of correlators and linearly combining their outputs. In aspect of hardware, it is necessary to construct a more practicable discriminator by employing as few correlators as possible. In Sect. 3.2, a proposed PCF with no side peaks for AltBOC(15,10) signals is investigated based on the quantitative analysis of Eq. 12.

3.2 Proposed Pseudo Correlation Function

The idea of the proposed method is not to subtract a CCF from the AltBOC(15,10) signal ACF. This new method employs two local SCS signals that non-coherently combine the output of the correlators in order to create an ideal triangular main peak with no side peaks function for tracking the AltBOC signals instead of the traditional ACF. In this method, we use a proposed PCF instead of the no-side-peak function, and the proposed PCF is defined as

$$R_{\mathrm{PCF}}^{\mathrm{Proposed}}(\tau) = \left| R_{\mathrm{CCF}}^{(1)}(\tau) \right| + \left| R_{\mathrm{CCF}}^{(2)}(\tau) \right| - \left| R_{\mathrm{CCF}}^{(1)}(\tau) + R_{\mathrm{CCF}}^{(2)}(\tau) \right| \tag{16}$$

where $R_{\mathrm{CCF}}^{(1)}(\tau)$ and $R_{\mathrm{CCF}}^{(2)}(\tau)$ are CCFs between AltBOC signal and two local SCS signals $s_{\mathrm{SCS}}^{(1)}\left(t; \boldsymbol{S}^{(1)}; f_c\right)$ and $s_{\mathrm{SCS}}^{(2)}\left(t; \boldsymbol{S}^{(2)}; f_c\right)$, respectively, in which $\boldsymbol{S}^{(1)}$ and $\boldsymbol{S}^{(2)}$ are the coded symbol sequence vectors of two local signals, respectively.

In order to obtain the proposed PCF, it is necessary to calculate the CCF of the received AltBOC signal and two local SCS signals. According to Eq. 12, the CCF of these signals can be expressed as

$$R_{\mathrm{CCF}}^{(1,2)}(\tau) = \frac{1}{8M} \sum_{k=0}^{M-1} \sum_{i=0}^{3} \sum_{l=0}^{M-1} \sum_{j=0}^{3} \left[\begin{array}{l} s_k^{\mathrm{AltBOC}} s_l^{(1,2)} \left(a_{1i} a_{1j} + a_{2i} a_{2j} + a_{3i} a_{3j} + a_{4i} a_{4j} \right) \times \\ \mathrm{Tri} \left[4 M f_c \left(\tau - \left((i-j) + 4(k-l) \right) \frac{T_s}{4} \right) \right] \end{array} \right] . \tag{17}$$

From Eq. 17, it can be seen that since the coded symbol sequence $s_k^{\text{AltBOC}} = (-1)^k$ of the received AltBOC(15,10) signal is known, the CCF entirely depends on the coded symbol sequences $s_l^{(1,2)}$ of local SCS signals spreading chip waveform. When considering designing the spreading chip waveform of local signals, since local signals do not relate to amplifying and transmitting in the receiver, they do not need to satisfy the request of constant modulus, and their spreading waveform should be easy to generate.

We assume that $s_l^{(1)} = -s_{M-l-1}^{(2)}$, then $R_{\text{CCF}}^{(1)}(\tau) = -R_{\text{CCF}}^{(2)}(-\tau)$ is easy to be obtained. To ensure the triangular shape without side-peaks, the proposed PCF must satisfy the following request:

$$\begin{cases} R_{\text{PCF}}^{\text{Proposed}}(\tau) \neq 0,\ \tau = 0 \\ R_{\text{PCF}}^{\text{Proposed}}(\tau) = 0,\ \tau \in [T_s, MT_s] \cup [-MT_s, -T_s] \end{cases}. \tag{18}$$

Due to the piecewise linear characteristic of CCF, if we use the absolute-magnitude operation to change the direction of lines on one side of the zero crossing point and following with linear combination, it is possible to obtain the proposed PCF without any side-peaks. Therefore, the $R_{\text{CCF}}^{(1)}(\tau)$ and $R_{\text{CCF}}^{(2)}(\tau)$ must satisfy

$$\begin{cases} R_{\text{CCF}}^{(1)}(\tau_0) = R_{\text{CCF}}^{(2)}(-\tau_0) = 0 \\ R_{\text{CCF}}^{(1)}(\tau_k) = R_{\text{CCF}}^{(2)}(\tau_k) = 0 \\ \left(\sum\limits_{l=0}^{M-1-k} s_l^{\text{AltBOC}} s_{l+k}^{(1,2)} A\right)\left(\sum\limits_{l=0}^{M-1-k} s_{l+k}^{\text{AltBOC}} s_l^{(1,2)} A\right) \geq 0 \\ \sum\limits_{k=0}^{M-1} \left(s_k^{(1,2)}\right)^2 = M \end{cases} \tag{19}$$

where $s_l^{\text{AltBOC}} = (-1)^l$, the parameter $A = \sum_{i=0}^{M-1} \sum_{j=0}^{M-1} \big(a_{1i}a_{1j} + a_{2i}a_{2j} + a_{3i}a_{3j} + a_{4i}a_{4j}\big)$, and $k = 0, 1, \ldots, M-1$.

Substituting Eq. 17 into Eq. 19, the coded symbol sequences of two local SCS signals can be obtained as follows when M is odd.

$$\begin{cases} \boldsymbol{S}^{(1)} = \left[\sqrt{\frac{M}{1+x^2}}, 0, \ldots, 0, -x\sqrt{\frac{M}{1+x^2}}\right]^{\text{T}} \\ \boldsymbol{S}^{(2)} = \left[x\sqrt{\frac{M}{1+x^2}}, 0, \ldots, 0, -\sqrt{\frac{M}{1+x^2}}\right]^{\text{T}} \end{cases}. \tag{20}$$

These two coded symbol sequence have been energy normalized and the shapes are identified by a parameter $x = -s_{M-1}^{(1)}/s_0^{(1)} = -s_0^{(2)}/s_{M-1}^{(2)}$, $x \in [01)$. Therefore, substituting Eqs. 20 and 17 into the expression of the proposed PCF Eq. 16, we can obtain a no-side-peak function $R_{\text{PCF}}^{\text{Proposed}}(\tau; x)$with a tunable parameter x.

The shape of the proposed PCF $R_{\text{PCF}}^{\text{Proposed}}(\tau; x)$ with $x = 0$ for AltBOC(15,10) signal ($M = 3$) is shown in Fig. 3. For comparison, the shapes of the AltBOC(15,10) signal ACF, SCPC method and DCF method are also given out. It can be seen that the shapes of the correlation function using the SCPC method is similar with that of BPSK(10) signal, i.e., the sharp main peak is destroyed, which means SCPC method removes all of the advantages of AltBOC signal tracking performance. For accurate delay tracking, preserving a sharp main peak of the ACF is a pre-requisite. The DCF method removes the side peaks completely while keeping the main peak, however, the amplitude of the main peak of this approach is degraded seriously, so this method is limited to be used in interference channel. In contrast to SCPC method and DCF method, the proposed PCF removes the side peaks while maintaining the

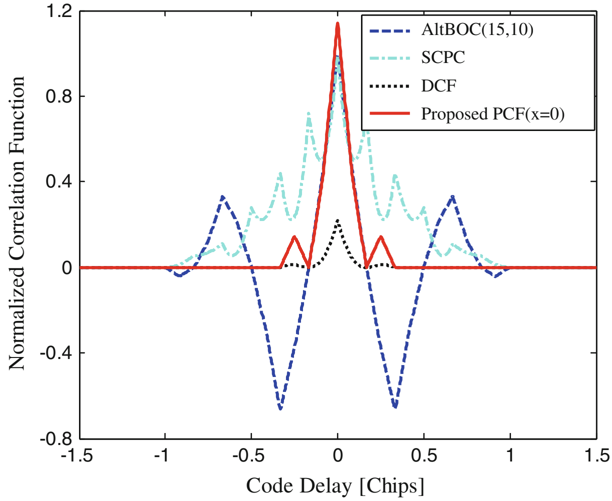

Fig. 3 AltBOC(15,10) signal normalized correlation functions comparison for traditional ACF, SCPC method, DCF method and the proposed PCF ($x = 0$), without front-end filter

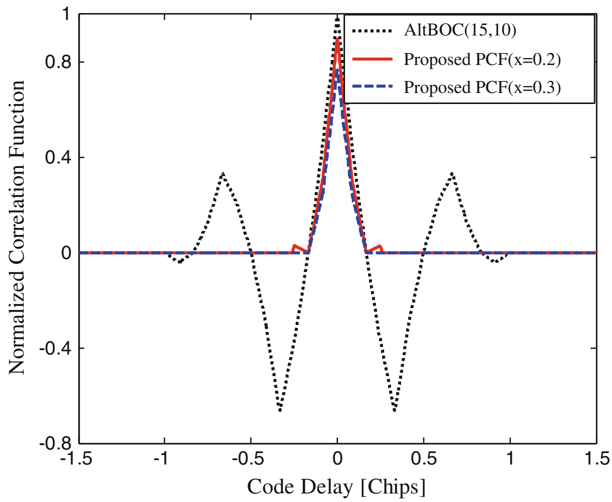

Fig. 4 AltBOC(15,10) signal normalized correlation functions comparison for traditional ACF and the proposed PCF ($x = 0.2$ and $x = 0.3$), without front-end filter

sharp shape of the main peak. Although the proposed PCF has two side peaks around ±0.25 chips, the magnitude of the side peaks is very small relative to the main peak. Therefore, it is not a bias threat in the design of the code delay discriminator, which will be seen in Fig. 8.

Figure 4 shows the shape of the proposed PCF $R_{\mathrm{PCF}}^{\mathrm{Proposed}}(\tau; x)$ with $x = 0.2$ and $x = 0.3$ for AltBOC(15,10) signal, without front-end filter. Figures 3 and 4 indicate that with the increase of x, the side peaks of the proposed PCF are completely removed, the half width and the magnitude of the main peak are decreased. It is important to note that $R_{\mathrm{PCF}}^{\mathrm{Proposed}}(0; x)$ will not always be one since the proposed PCF is not a real ACF.

In reality, one has to take into account the impact of the front-end filter on each CCF. The impact of a front-end filter with a 75 MHz double-sided bandwidth on the AltBOC(15,10)

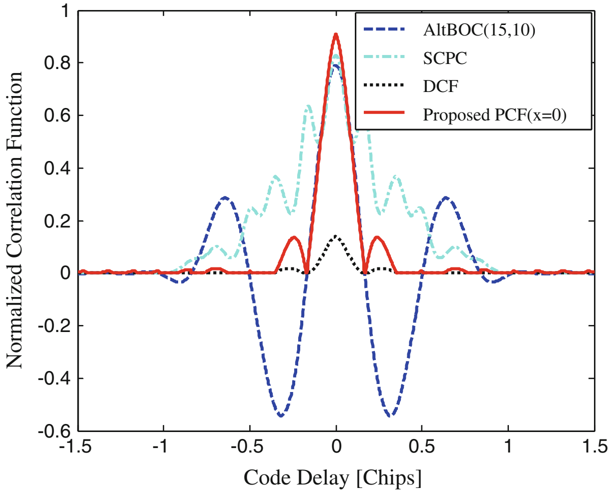

Fig. 5 AltBOC(15,10) signal normalized correlation functions comparison for traditional ACF, SCPC method, DCF method and the proposed PCF ($x = 0$), with 75 MHz front-end filter

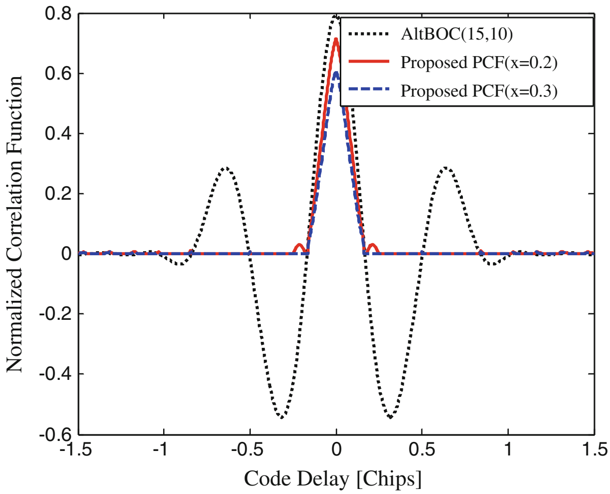

Fig. 6 AltBOC(15,10) signal normalized correlation functions comparison for traditional ACF and the proposed PCF ($x = 0.2$ and $x = 0.3$), with 75 MHz front-end filter

signal are shown in Figs. 5 and 6 with respect to Figs. 3 and 4. Analyzing Figs. 5 and 6, it can be noted that even the front-end filter makes the shapes of the correlation functions $R_{\text{CCF}}^{(1)}(\tau)$ and $R_{\text{CCF}}^{(2)}(\tau)$ change, the proposed PCF $R_{\text{PCF}}^{\text{Proposed}}(\tau; x)$ still have no side peaks. Therefore, the proposed PCF can be used in the discriminator of the NEML tracking loop instead of the traditional ACF.

3.3 Unambiguous Tracking Method Based on Proposed PCF

Since the proposed PCF with no side peaks is obtained, as a consequence, a new architecture of the non-coherent NEML tracking loop, based on the proposed PCF can be presented. This

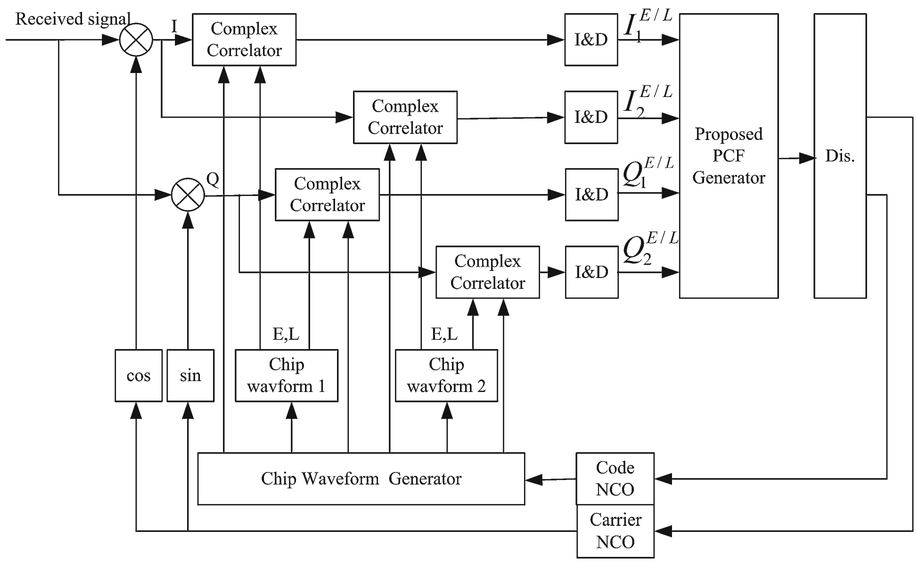

Fig. 7 New DLL architecture based on proposed PCF

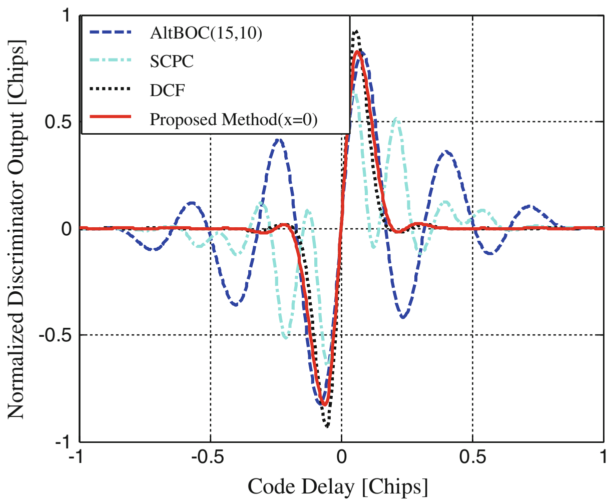

Fig. 8 Normalized discriminator outputs comparison for traditional AltBOC(15,10) signal, SCPC method, DCF method and the proposed method ($x = 0$), with 75 MHz front-end filter

new delay lock loop (DLL) architecture is depicted in Fig. 7. The received AltBOC(15,10) signal is first multiplied with the local carrier, and then down converted to baseband in-phase (I) and quadrature-phase (Q) signals. The local chip waveform generator generates early and late spreading chip waveform with a spacing Δ between them. Each chip waveform is modulated by the $s_{\mathrm{SCS}}^{(1)}\left(t; \boldsymbol{S}^{(1)}; f_c\right)$ and $s_{\mathrm{SCS}}^{(2)}\left(t; \boldsymbol{S}^{(2)}; f_c\right)$ independently. Then the local sub-carriers and spreading chip waveforms are complex correlated with the baseband I and Q signals in complex correlators. The results of those multipliers are resampled by the integrate and dump accumulators with the duration time T, and the proposed PCF can be expressed as

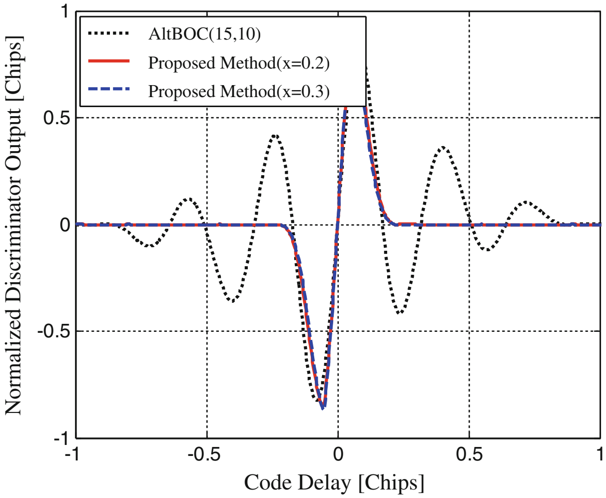

Fig. 9 Normalized discriminator outputs comparison for traditional AltBOC(15,10) signal and the proposed method with $x = 0.2$ and $x = 0.3$, with 75 MHz front-end filter

$$R_{\mathrm{PCF}}^{\mathrm{Proposed}}(\tau; x) = \sqrt{I_1^2 + Q_1^2} + \sqrt{I_2^2 + Q_2^2} - \sqrt{(I_1 + I_2)^2 + (Q_1 + Q_2)^2}. \tag{21}$$

The final result of the discriminator output $D_{\mathrm{PCF}}^{\mathrm{Proposed}}(\tau; x)$ based on the proposed PCF is given as

$$D_{\mathrm{PCF}}^{\mathrm{Proposed}}(\tau; x) = \left(\left(R_{\mathrm{PCF}}^{\mathrm{Proposed}}(\tau; x)\right)^E\right)^2 - \left(\left(R_{\mathrm{PCF}}^{\mathrm{Proposed}}(\tau; x)\right)^L\right)^2 \tag{22}$$

where the subscripts of $\left(R_{\mathrm{PCF}}^{\mathrm{Proposed}}(\tau; x)\right)^E$ and $\left(R_{\mathrm{PCF}}^{\mathrm{Proposed}}(\tau; x)\right)^L$ indicate early (E) and late (L), respectively.

Figure 8 shows the new discriminator output $D_{\mathrm{PCF}}^{\mathrm{Proposed}}(\tau; x)$ with $x = 0$ for AltBOC(15,10) modulation signal with a 75 MHz double-sided bandwidth front-end filter, and for an early-late spacing of $\Delta = 0.1$ chips. It also shows the discriminator characteristic curves of the NEML loop which uses the traditional AltBOC(15,10) ACF, SCPC method and DCF method. It is interesting to note that the discriminator based on the proposed PCF with $x = 0$ removes the false lock points completely, and the DCF method achieves the same performance with the proposed method. Unfortunately, the discriminator output of the SCPC method still has some false lock points, which would result in intolerable biased measurements.

Figure 9 shows the new discriminator output $D_{\mathrm{PCF}}^{\mathrm{Proposed}}(\tau; x)$ with $x = 0.2$ and $x = 0.3$ for AltBOC(15,10) modulation signal using a 75 MHz double-sided bandwidth front-end filter, and for an early-late spacing of $\Delta = 0.1$ chips. It can be seen that whether the $D_{\mathrm{PCF}}^{\mathrm{Proposed}}(\tau; x)$ with $x = 0.2$ or the $D_{\mathrm{PCF}}^{\mathrm{Proposed}}(\tau; x)$ with $x = 0.3$, by using the proposed PCF instead of AltBOC ACF, the new DLL based on the proposed PCF completely removes the false lock points.

It is also important to note that both the baseline width and the peak height of the proposed PCF are related with the parameter x. Changing the value of x can change the linear range of the discriminator and the slope of the discriminator characteristic curve.

Now that the principles of the proposed method have been explained in detail and its unambiguous property has been shown, it is important to study the impact of the main sources of error on the code tracking performance to ensure that it does not imply significant drawbacks. As a consequence, the effect of multipath is investigated in the following section.

4 Impact of Multipath on Proposed Method

Multipath has been considered as a major sources of measurement error in GNSS signal tracking, which is due to the mixing, at the antenna level, of the direct signal with delayed replicas of the same signal, it distorts signal modulation and degrades accuracy [15,16].

This analysis assumes a multipath scenario with a single reflector. Although the common multipath environment involves multiple rays, the single ray is the most common scenario for the evaluation of the general multipath rejection performance [17]. The maximum pseudorange measurement errors due to one-path specular reflection with a relative amplitude of -6 dB are evaluated, and the early-late spacing $\Delta = 0.1$ chips.

Figure 10 presents the performance of the multipath mitigation of the new DLL based on the proposed PCF ($x = 0$) for AltBOC(15,10) signal with 75 MHz front-end filter bandwidth. For comparison, the traditional AltBOC signal tracking method, BPSK-like method, SCPC method and DCF method are also given out in Fig. 10.

Form Fig. 10, it can be seen that SCPC method achieves a better multipath mitigation performance than the other methods, However, SCPC method can not remove the false lock points completely, which would result in larger bias pseudo-range measurements than that of multipath induced, as illustrated in Fig. 8. The new DLL based on the proposed method has a better performance in terms of mitigation of short-, medium- and long-delay multipath than the BPSK-like method. For multipath delays within [0; 0.3] chips, the proposed method seems to mitigate multipath slightly better than the other methods, especially for the DCF method, while for multipath delays within [0.6; 1] chips, it is opposite. This phenomenon and the fact that the medium- and long-delay multipath mitigation performance of the proposed method is not very ideal seem incompatible with the fact that the proposed PCF has a

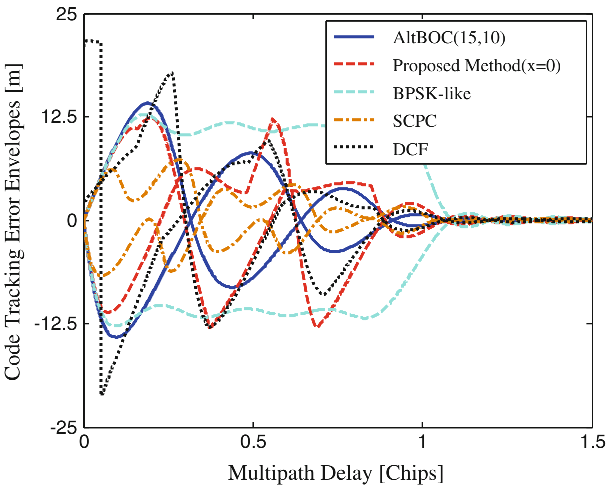

Fig. 10 Code tracking multipath envelopes comparison for AltBOC(15,10), the proposed method, BPSK-like method, SCPC method, and DCF method, with 75 MHz front-end filter

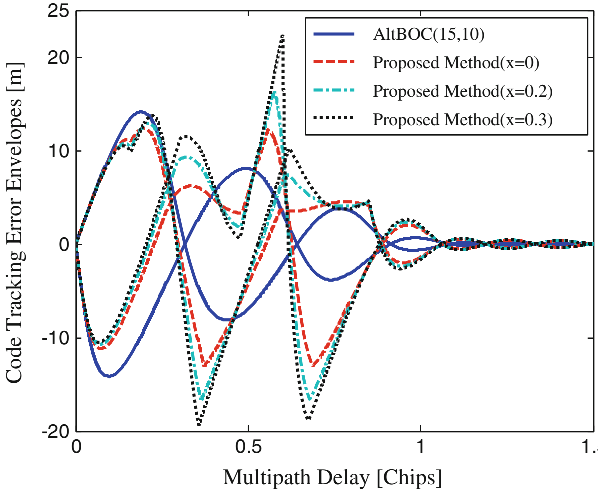

Fig. 11 Code tracking multipath envelopes comparison for AltBOC(15,10), the proposed method with $x = 0.2$ and $x = 0.3$, with 75 MHz front-end filter

sharp main peak with no side peak and that increasing x can decrease the half width of the main peak, as illustrated in Fig. 4. However, one should note that the proposed PCF is based on the non-coherent combination of several CCFs which do not have narrow peaks and are more susceptible to multipath. Those CCFs with dissatisfactory shapes worsen the multipath mitigation performance of the proposed method.

Figure 11 shows the performance of the multipath mitigation of the new DLL based on the proposed PCF with $x = 0.2$ and $x = 0.3$ for AltBOC(15,10) signal using a 75 MHz front-end filter bandwidth. The figure indicates that with the decrease of x, the multipath mitigation performance of the proposed method is improved.

5 Conclusions

This paper derives the analytical expression of the CCF of two SCS signals and presents a new tracking method, dedicated to AltBOC(15,10) signals, that has been shown to be reliably unambiguous. It can be adapted to different types of front-end filters (wide or narrow) in order to achieve the best tracking performance. The proposed method uses a proposed PCF with a tunable parameter x for tracking instead of the traditional ACF. It has been shown that the proposed PCF completely removes the side peaks, and the proposed method has no false lock points in the discriminator output. Moreover, for AltBOC(15,10) signal tracking, the proposed method has an average multipath mitigation performance compared with others unambiguous methods.

In the aspect of hardware, the proposed method is practicable and requires only four complex correlators as well as SCPC method, which is less than DCF method. Moreover, it has an equivalent form to the proposed method whose correlators and modulators are easily implemented via logic circuits. Besides, the proposed method can be expanded to solve even and odd AltBOC(m, n) modulation ambiguity problem.

Future work will focus on the quantitative analysis of the thermal noise performance under this method. It is useful for the design of the tracking loop.

Acknowledgments This work was supported by National Nature Science Foundation of China (No. 61179004, 61179005).

References

1. United Nations. (2010). Current and planned global and regional navigation satellite systems and satellite-based augmentations systems. In *International committee on global navigation satellite systems provider's forum*. New York.
2. European Union. (2010). European GNSS (Galileo) open service signal in space interface control document. *Document subject to terms of use and disclaimers p. II–III OD SIS ICD, Issue 1.1*.
3. Tang, Z. P., Zhou, H. W., & Wei, J. L., et al. (2011). TD-AltBOC: A new COMPASS B2 modulation. *Science China Physics, Mechanics & Astronomy, 54*(6), 1014–1021.
4. Kaplan, E. D., & Hegarty, C. (2006). *Understanding GPS: Principles and applications*. Artech House Mobile Communications Series.
5. Nagaraj, C. S., Andrew G. D., & Chris, R. (2011). On efficient wideband GNSS signal design. In *Proceeding of ION international technical meeting* (pp. 401–410), San Diego, CA.
6. Julien, O., Macabiau, C., & Issler, J. (2009). Ionospheric delay estimation strategies using Galileo E5 signals only. In *Proceeding of ION international technical meeting* (pp. 3128–3141), Savannah, GA.
7. Nagaraj, C. S., & Andrew G. D. (2008). An analysis of Galileo E5 signal acquisition strategies. In *Proceeding of the European Nav Conference, ENC GNSS* (pp. 186–190), Toulouse.
8. Kim, S., Yoo, S., Yoon, S., & Kim, S. Y. (2009). AltBOC and CBOC correlation functions for GNSS signal synchronization. *Computer Science, 5593*(2009), 325–334.
9. Yao, Z., Lu, M., & Feng, Z. (2010). Pseudo-correlation-function-based unambiguous tracking technique for Sine-BOC signals. *IEEE Transaction on Aerospace and Electronic System, 46*(4), 1782–1796.
10. Yao, Z., & Lu, M. (2011). Side-peaks cancellation analytic design framework with applications in BOC signals unambiguous processing. In *Proceeding of ION international technical meeting* (pp. 775–785), San Diego, CA.
11. Halunga, S. C., Vizireanu, D. N., & Fratu, O. (2010). Imperfect cross-correlation and amplitude balance effects on conventional multiuser decoder with turbo encoding. *Digital Signal Processing, 20*(1), 191–200.
12. Halunga, S. C., & Vizireanu, D. N. (2010). Performance evaluation for conventional and MMSE multiuser detection algorithms in imperfect reception conditions. *Digital Signal Processing, 20*(1), 166–178.
13. Rebeyrol, E., Macabiau, C., Lestarquit, L., et al. (2005). BOC power spectrum densities. In *Proceeding of ION-NTM* (pp. 769–778), Long Beach, California.
14. Rodriguez, J. A. (2008). *On generalized signal waveforms for satellite navigation*. Munich, Germany: University FAF Munich.
15. Aleksandar, J., Youssef T., Cyril, B., & Pierre, F. (2010). Multipath mitigation techniques for CBOC, TMBOC and AltBOC signals using advanced correlators architectures. In *Proceeding of ION PLANS* (pp. 1127–1136), Indian Wells, CA, USA.
16. Nagaraj, C. S. (2009). Code phase multipath mitigation by exploiting the frequency diversity in Galileo E5 AltBOC. In *Proceedig of ION international technical meeting* (pp. 3219–3233), Savannah, GA.
17. Rouabah, K., Chikouche, D., Bouttout, F., Harba, R., & Ravier, P. (2011). GPS/Galileo multipath mitigation using the first side peak of double delta correlator. *Wireless Personal Communications, 60*(2), 321–333.

Author Biographies

Huihua Chen was born in Fujian, China in 1983. He received his M.Sc. from Xi'an Research Institute of High Technology, Xi'an, China in 2009. He is currently working toward the Ph.D. degree at Xi'an Research Institute of High Technology. His research interests include satellite navigation signal structure design and signal processing.

Rong Wang was born in Shanxi, China in 1983. He received his M.Sc. from Xi'an Research Institute of High Technology, Xi'an, China in 2007. He is currently working toward the Ph.D. degree at the department of automation, Tsinghua University, Beijing, China. His research interests include satellite navigation signal structure design and signal processing.

Weimin Jia was born in Hebei, China in 1971. She received her Ph.D. degree from Xi'an Research Institute of High Technology, Xi'an, China in 2007. She is an associate professor in the Department of Communication Engineering, Xi'an Research Institute of High Technology, Xi'an, China. Her current research interests include Sat-COM, Spreading Communication.

Jiawei Ren was born in Henan, China in 1985. He received his M.Sc. from Xi'an Research Institute of High Technology, Xi'an, China in 2010. He is currently working toward the Ph.D. degree at Xi'an Research Institute of High Technology. His research interests include satellite navigation signal structure design and signal processing.

Minli Yao was born in Shanxi, China in 1966. He obtained his M.Sc. from Xi'an Research Institute of High Technology, Xi'an, China in 1992 and Ph.D. degree from Xi'an Jiao Tong University, Xi'an China in 1999, respectively. He is currently a professor at the Department of Communication Engineering, Xi'an Research Institute of High Technology, Xi'an, China. His research interests include satellite navigation signal structure design and signal processing, Sat-COM, and Spreading Communication.